Journal of Industrial and Engineering Chemistry 20 (2014) 830–840

Contents lists available at SciVerse ScienceDirect

Journal of Industrial and Engineering Chemistry

journal homepage: www.elsevier.com/locate/jiec

Optimized and functionalized paper sludge activated with potassium fluoride for single and binary adsorption of reactive dyes

M. Auta, B.H. Hameed *

School of Chemical Engineering, Engineering Campus, Universiti Sains Malaysia, 14300 Nibong Tebal, Penang, Malaysia

ARTICLE INFO

Article history:
Received 8 April 2013
Accepted 7 June 2013
Available online 15 June 2013

Keywords:
Paper sludge
Potassium fluoride
Extended Langmuir model
Functionalization
Activated carbon

ABSTRACT

The yield and adsorption uptake of optimized paper sludge activated carbon (PSAC) prepared using potassium fluoride as alternative chemical activation agent was investigated. The PSAC was functionalized with ethylenediamine (FPSAC) and both adsorbents were used for single and binary adsorption of Reactive orange 16 (RO16) and Reactive blue 19 (RB19). Effect of pH on the adsorption process, equilibrium, kinetics, isotherm and thermodynamic studies were carried out. Optimum PSAC preparation parameters were: activation temperature, X_1 = 810 °C; activation time, X_2 = 105 min; and impregnation ratio, X_3 = 0.95 which gave adsorption uptake of 178 and 158 mg/g for RO16 and RB19, respectively.
© 2013 The Korean Society of Industrial and Engineering Chemistry. Published by Elsevier B.V. All rights reserved.

1. Introduction

Development of mechanisms and processes for treating effluents has received tremendous attention in the past decades with a view to preserving our environment that is increasingly abused by anthropogenic effects. Among various classes of effluents is the cosmopolitan dye wastewater that is a bane to the entire ecosystem. Dye effluents common characteristics include high biochemical oxygen demand, chemical oxygen demand, heavy metals, dye compounds, salts, surfactants and some solid particles. It is carcinogenic, mutagenic and affects the reproductive system, liver and kidney of humans. Dyes categories includes acidic, azoic, basic, direct, disperse, ingroin, mordant, reactive, sulphur and vat dyes; they can be generally classified into anionic, cationic and nonionic dyes [1,2]. Coagulation, membrane separation techniques, advance oxidation, electrochemical processes, adsorption process are among numerous ways of treating dye wastewaters but they have limitations. Adsorption process is outstanding due to its simplicity and efficiency but its major challenge is the commercial activated carbon often used that is overpriced [3,4]. The nature of real textile wastewater calls for change of research approach from single to binary adsorption of dye molecules [1].

Tailoring of biosolids from sludge for adsorption purpose is gaining interest of many environmental researchers. Biosolid adsorbents have helped to augment other low cost agricultural and clay materials that have been researched into as alternative to expensive commercial activated carbon. The need for valorization of sludge is due to its large generation and poor disposal methods. Common methods of sludge disposal include its usage as fertilizer which has been hampered by legislation in recent time; incineration-very expensive; and, recycling for landfill-poor public image [5,6]. Many attempts have been made to convert sludge into activated carbon with much success and a comprehensive review has been reported. The major challenge in the field involves discovering an alternative activation agent, most effective chemical activation technique optimization, tailoring of surface chemistry and activation technique for selective adsorption of adsorbents and the need for evaluation of economic viability of large scale production of sludge base activated carbons [7].

The most effective chemical activation agent for development of activated carbon from carbonaceous materials is potassium hydroxide (KOH) [7,8]. It has been used to produce activated carbon with high surface area of 1882 m^2/g [9], 1686 m^2/g [10], and 1002 m^2/g [11]. The efficacy of KOH is as a result of numerous developmental stages involved in its reaction with the carbonaceous material which aids in porosity and surface area development [12,13]. The high reactive nature of potassium makes it not to be found naturally in its elemental state or concentrated in one location. Its common compounds include potassium hydroxide (KOH), potassium carbonate (K_2CO_3), potassium fluoride (KF), potassium acetate (CH_3COOK) and potassium nitrate (KNO_3) among others.

In recent years fluorine has been used as good additives for base-assisted reaction, they exert strong basicity by their high hydrogen bonding ability to water molecules by hydration [14–16]. Fluorine content of a fluorinated carbon (CF) – a product of reaction between fluorine and carbon material can be eliminated as CF compound through heating of the sample above 750 °C [17].

* Corresponding author. Tel.: +60 45996422; fax: +60 45941013.
E-mail address: chbassim@eng.usm.my (B.H. Hameed).

1226-086X/$ – see front matter © 2013 The Korean Society of Industrial and Engineering Chemistry. Published by Elsevier B.V. All rights reserved.
http://dx.doi.org/10.1016/j.jiec.2013.06.013

Potassium fluoride dissociates into K^+ and F^- in polar solvents and so the potassium metal ion hydrates with OH^- molecules of water exothermically to form KOH [18]. Potassium fluoride has been used as source of KOH in previous studies [14,19]. Therefore reaction of KF with carbonaceous material at high activation temperature will result into global reaction of chemical activation with KOH given in Eq. (1) [9,20,21]. Compounds of fluorides such as HF, KF, NH_4F, NH_4HF_2 have been used for modification of clay minerals to increase their surface area and porosity [22]; and for enhancement of adsorption, activated carbon from paper sludge was post treated with HF by previous researchers [23].

$$6KOH + 2C \rightleftharpoons 2K_2CO_3 + 2K + 3H_2 \quad (1)$$

The affinity between sorbate and sorbent is paramount in adsorption processes since some porous adsorbents may not have attraction for the pollutant. To promote adsorption activities of an adsorbent, its external and internal surface can be modified to increase attraction force of targeted adsorbate toward it. Modification or functionalization of adsorbent helps to improve the mechanical properties of the sorbent, good selectivity toward trace pollutants and generally enhances sorption capacity of adsorbents [24–26].

This study is aimed at developing new method of preparing activated carbon from paper sludge through investigating the use of potassium fluoride as activation agent and optimization of the preparation parameters. It also involved functionalization of the paper sludge activated carbon (PSAC) with ethylenediamine (EDA) to enhance its adsorption for single and binary Reactive orange 16 (RO16) and Reactive blue 19 (RB19) dyes from aqueous solution. Kinetics, equilibrium, isotherm and thermodynamics studies; and effect of initial concentration on adsorption experiments were carried out.

2. Materials and methods

2.1. Materials

Reactive blue 19 (RB19) and Reactive orange 16 (RO16) were supplied by Aldrich and Sigma chemicals, Malaysia; their chemical structures are presented in Fig. 1. Sodium hydroxide (NaOH), hydrochloric acid (HCl), ethylenediamine (EDA) and potassium fluoride (KF) were supplied by Merck Company Malaysia and used without further purification. Paper sludge (PS) was obtained from local paper company, Malaysia; it was dried, ground and stored for usage. The PS elemental analysis (%) gave C = 24.18, H = 0.83, N = 1.27, S = 0.75; while its proximate analysis revealed that the moisture content, volatile matter, fixed carbon and ash content all in percentage were 14.35, 38.12, 24.97 and 22.56, respectively

2.2. Preparation of paper sludge activated carbon

Three parameters such as activation temperature (650–850 °C), activation time (30–120 min) and impregnation ratio IR (ratio of mass of potassium fluoride to mass of paper sludge char) (0.50–2.0) were selected for optimization in preparation of activated carbon from the paper waste. The ground paper sludge was sieved into 200–500 μm particle sizes and loaded in stainless steel vertical tubular crucible into a furnace for carbonization. The furnace temperature was set at 700 °C for 2 h, heating rate of 10 °C/min and 150 cm^3/min nitrogen (95.95%) was flown through the furnace. The char prepared was mixed with the activating agent (potassium fluoride) in a plastic container as stipulated by the design of experiment (DOE) Table 1.

The impregnated paper sludge char was dried in an oven at 110 °C overnight. It was transferred to the furnace for activation programmed in accordance with the DOE Table 1 under similar conditions as carbonization process. The activated sample was washed with water until the supernatant was at neutral pH (6.8–7); the presence of fluoride was tested by pouring the supernatant on glass to observe possibility of etching effect and the dried sample was treated with concentrated sulfuric acid for possible steamy acidic fumes which indicates presence of halides on solids. Then the activated sample was washed with 5 M HCl solution and later washed with water until neutrality (pH 6.5–7) was attained before further usage.

2.3. Design of experiment using response surface methodology

Central composite design (CCD), a segment of response surface methodology was used to optimize the selected preparation parameters (activation temperature, impregnation ratio and activation time) of paper sludge activated carbon (PSAC). The responses for this optimization were adsorption uptake and percentage yield. These parameters were correlated with the responses through empirical model using optimal predictor quadratic equation model given as [27]:

$$Y = b_0 + \sum_{i=1}^{n} b_i x_i + \left(\sum_{i=1}^{n} b_{ii} x_i\right)^2 + \sum_{i=1}^{n-1}\sum_{j=i+1}^{n} b_{ij} x_i x_j \quad (2)$$

where Y is the predicted response, b_0 is the constant coefficients, b_{ii} the quadratic coefficients, b_{ij} the interaction coefficients and x_i, x_j are the coded values of the variables considered.

Design Expert software (statistical) version 6.0.6 (STAT-EASE Inc., Minneapolis, USA) statistical software was used for fitting the equation developed through regression analysis and for evaluation of the significance of the resulting equation.

2.4. Yield of PSAC and its adsorption uptake of RO16/RB19

The percentage yield of the PSAC was calculated using Eq. (3):

$$\text{Yield}\,(\%) = \frac{\text{mass (g) of dried PSAC prepared}}{\text{mass (g) dried precursor used}} \times 100 \quad (3)$$

The adsorbate (RO16 and RB19) initial concentration of 200 mg/L (100 mL) was measured into a set of 250 mL Erlenmeyer flasks and 0.1 g of PSAC was added before placing the flasks in isothermal water-bath shaker (140 rpm) set at 30 °C for 24 h. The residual

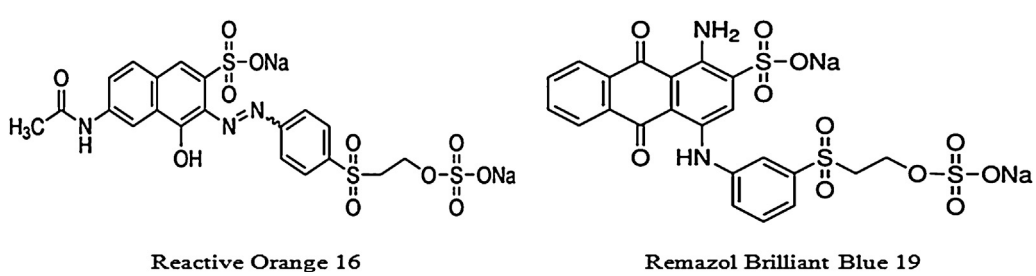

Fig. 1. Chemical structure of RO16 and RB19.

Table 1
Experimental design matrix for paper sludge activated carbon preparation.

Run	PSAC preparation parameters			Adsorption capacity (Y_1) (mg/g)	Adsorption capacity (Y_2) (mg/g)	Yield (Y_3) (%)
	Activation temperature (X_1) (°C)	Activation time (X_2) (min)	KF impregnation ratio (X_3)			
1	691 (−1)	48 (−1)	0.80 (−1)	34.16	28.73	13.45
2	809 (+1)	48 (−1)	0.80 (−1)	175.24	156.35	10.30
3	691 (−1)	102 (+1)	0.80 (−1)	49.25	50.97	21.63
4	809 (+1)	102 (+1)	0.80 (−1)	192.88	169.41	9.17
5	691 (−1)	48 (−1)	1.70 (+1)	26.54	31.56	16.30
6	809 (+1)	48 (−1)	1.70 (+1)	87.56	55.13	11.90
7	691 (−1)	102 (+1)	1.70 (+1)	19.73	16.21	15.96
8	809 (+1)	102 (+1)	1.70 (+1)	66.56	60.06	3.67
9	650 (−1.682)	75 (0)	1.25 (0)	12.46	6.11	18.00
10	850 (+1.682)	75 (0)	1.25 (0)	130.73	140.71	3.87
11	750 (0)	30 (−1.682)	1.25 (0)	123.00	113.07	11.68
12	750 (0)	120 (+1.682)	1.25 (0)	130.41	134.44	10.11
13	750 (0)	75 (0)	0.50 (−1.682)	140.35	125.00	14.71
14	750 (0)	75 (0)	2.00 (+1.682)	13.69	14.33	8.35
15	750 (0)	75 (0)	1.25 (0)	98.00	82.57	12.05
16	750 (0)	75 (0)	1.25 (0)	110.66	97.31	11.50
17	750 (0)	75 (0)	1.25 (0)	120.67	99.04	11.91
18	750 (0)	75 (0)	1.25 (0)	119.78	89.67	10.52
19	750 (0)	75 (0)	1.25 (0)	131.36	110.53	10.49
20	750 (0)	75 (0)	1.25 (0)	119.97	100.60	12.51

concentration in the flasks after attainment of equilibrium was determined using UV–vis spectrophotometer (Shimadzu UV-1601 spectrophotometer, Japan) at maximum wavelength of 493 for RO16 and 591 for RB19. The adsorption uptake was calculated as follows:

$$q_e = \frac{(C_0 - C_e)V}{w} \tag{4}$$

where C_0 and C_e (mg/L) are the liquid-phase concentration of the RO16/RB19 at initial and at equilibrium, respectively; V (L) is the volume of the solution; and W (g) is the mass of the adsorbent.

2.5. Functionalization of PSAC with ethylenediamine

Modification of optimized PSAC with ethylenediamine (EDA) was carried out by adding 2 g of PSAC to 150 mL of 0.05 M EDA solution in 250 mL Erlenmeyer flask. The flask was placed in an isothermal water-bath shaker (140 rpm) set at 50 °C for 6 h. The modified PSAC was recovered after cooling to room temperature and washed with distilled water to neutrality point, dried in an oven and then packaged for use. The EDA modified PSAC was tagged FPSAC.

2.6. Characterization of PSAC

Brunauer–Emmett–Teller (BET) surface area and porosity of the PSAC was carried out using Micrometrics (ASAP 2000, US) nitrogen adsorption–desorption method, morphological structure of the raw paper sludge and the PSAC snapped using scanning electron microscopy (SEM) (Model Leo Supra 50VP Field Emission, UK) and the adsorbents surface chemistry before and after single and binary adsorption of RO16 and RB19 were determined with Fourier transform infrared (FTIR) spectroscope (FTIR-2000, PerkinElmer). The PSAC and FPSAC surface acidity through Boehm titration and pH zero point of charge were determined as previously reported [3].

2.7. Equilibrium and kinetic adsorption experiment

The single adsorption experiment commenced with preparation of 500 mg/L each of RO16 and RB19 by dissolving appropriate mass of the dyes in distilled water. To a set of 250 mL Erlenmeyer flasks, 100 mL of initial adsorbate concentration of 50–350 mg/L range were introduced and 0.1 g of PSAC/FPSAC was added. The flasks were swirled for perfect contact between the sorbate and adsorbent after which, they were placed in isothermal water-bath shaker set at 140 rpm, 30 °C for 24 h. Prior to equilibrium condition, the residual sorbate concentration was measured at intervals of time with the aid of UV–vis spectrophotometer (Shimadzu UV-1601 spectrophotometer, Japan) at maximum wavelength of 493 (λ_1) for RO16 and 591 (λ_2) for RB19. The isothermal settings of the water-bath shaker were adjusted to 40 and 50 °C and the entire process was repeated. The uptake of the adsorbate per unit mass of the adsorbent at any time t was determined as follows:

$$q_t = \frac{(C_0 - C_t)V}{W} \tag{5}$$

where C_0 and C_t (mg/L) are the liquid-phase concentration of the RO16/RB19 at initial and at any time t, respectively; V (L) is the volume of the solution; and W (g) is the mass of the adsorbent.

A pH range of 2–12 was adjusted with either 0.1 M HCl or NaOH to study the effect of pH on adsorption of RO16/RB19 by the adsorbent.

For binary adsorption systems, RO16 and RB19 were denoted '1' and '2', respectively; and mixture of the dyes as 'RORBB' throughout the study. The industrial practice of equal mass concentrations of preparing binary system dye mixture was adopted [28]. Equal concentration of RO16 and RB19 were measured throughout in preparation of initial sorbate concentration. At RO16 and RB19 wavelengths of λ_1 and λ_2, the residual sorbate concentration in the solution was determined to give optical densities of d_1 and d_2, respectively; the equation described by Choy et al. [29] was used:

$$C_{e,1} = \frac{K_{2,2}d_1 - K_{2,1}d_2}{K_{1,1}K_{2,2} - K_{1,2}K_{2,1}} \tag{6}$$

$$C_{e,2} = \frac{K_{2,1}d_2 - K_{1,2}d_1}{K_{1,1}K_{2,2} - K_{1,2}K_{2,1}} \tag{7}$$

In competitive adsorption, the wrong use of Langmuir model parameters q_m and K_L of mono-sorbate condition for binary systems has been corrected. The mathematical equations proposed for determining Langmuir model q_m and K_L parameters for binary

systems [28] are:

$$q_{m(\text{bin})} = q_{m,1(\text{bin})}\theta_1 + q_{m,2(\text{sin})}\theta_2 \tag{8}$$

$$K_{L,1(\text{bin})} = K_{L,1(\text{sin})}\exp^{(-\theta_2/\theta_1)} \tag{9}$$

$$K_{L,2(\text{bin})} = K_{L,2(\text{sin})}\exp^{(-\theta_1/\theta_2)} \tag{10}$$

where θ_1 and θ_2 are the fractional loading of RO16 and RB19, respectively on the surface of the adsorbent.

Substitution of Eqs. (8)–(10) into the extended Langmuir equation (11) [30] gives Eqs. (12) and (13):

$$q_{e,i} = \frac{q_{m,i}K_{L,i}C_{e,i}}{1 + \sum_{j=1}^{n} K_{L,i}C_{e,i}} \tag{11}$$

$$q_{e,1(\text{bin})}\frac{(q_{m,1(\text{sin})}\theta_1 + q_{E,z(\text{sin})}\theta_z)K_{L,1(\text{sin})}\exp^{(-\theta_z/\theta_1)}C_{e,1(\text{bin})}}{1 + K_{L,1(\text{sin})}\exp^{(-\theta_z/\theta_1)}C_{e,1(\text{bin})} + K_{L,z(\text{sin})}\exp^{(-\theta_1/\theta_z)}C_{e,z(\text{bin})}} \tag{12}$$

$$q_{e,2(\text{bin})} = \frac{(q_{m,1(\text{sin})}\theta_1 + q_{m,z(\text{sin})}\theta_z)K_{L,2(\text{sin})}\exp^{(-\theta_1/\theta_z)}C_{e,z(\text{bin})}}{1 + K_{L,1(\text{sin})}\exp^{(-\theta_z/\theta_1)}C_{e,1(\text{bin})} + K_{L,z(\text{sin})}\exp^{(-\theta_1/\theta_z)}C_{e,z(\text{bin})}} \tag{13}$$

2.8. Desorption and reusability of PSAC and FPSAC

The recovered PSAC/FPSAC (0.10 g) from 200 mg/L of RO16 or RB19 at the optimum adsorption pH was rinsed slightly with distilled water to remove the adsorbed dye. It was transferred into 100 mL NaOH solution (pH 10), agitated for 10 h and then recovered to complete the desorption process. Reusability experiment was carried out using 200 mg/L RO16 or RB19 in a similar manner as described in Section 2.7; the entire process was repeated three times.

3. Results and discussion

3.1. Regression model equation development

Quadratic model and two-factor interaction (2FI) were developed for PSAC adsorption capacity and PSAC percentage yield as suggested by CCD. The range of PSAC yield obtained was 3.67–21.63% which had adsorption uptake of 13.69–192 mg/g for RO16 and 6.11–169.41 mg/g for RB19. The coded resulting empirical models for adsorption of RO16 (Y_1), adsorption of RB19 (Y_2) and yield of PSAC (Y_3) are:

$$\begin{aligned} Y_1 = {} & 117.02 + 43.31X_1 + 1.27X_2 - 33.99X_3 - 17.81X_1^2 \\ & + 1.67X_2^2 - 15.89X_3^2 - 1.46X_1X_2 - 22.11X_1X_3 \\ & - 7.57X_2X_3 \end{aligned} \tag{14}$$

$$\begin{aligned} Y_2 = {} & 97.18 + 39.53X_1 + 4.45X_2 - 31.39X_3 - 11.88X_1^2 \\ & + 5.92_2^2 - 13.21_3^2 + 1.39X_1X_2 - 22.33X_1X_3 - 5.72X_2X_3 \end{aligned} \tag{15}$$

$$\begin{aligned} Y_3 = {} & 11.90 - 4.11X_1 + 0.30X_2 - 1.28X_3 - 2.15X_1X_2 \\ & - 0.13X_1X_3 - 1.95X_2X_3 \end{aligned} \tag{16}$$

The ANOVA for the yield of the PSAC revealed a good agreement between the actual experimental and the predicted values as their correlation coefficient square R^2 was 0.943, and the outlier values were within threshold limit. The model F-value of 36.06 implied that it was significant and had only a 0.01% chance that its magnitude could occur due to noise (induced variation under normal operating conditions by uncontrollable factors). As expected, non-significant lack of fit was obtained with lack of fit F-value = 2.85 implying its non-significance relative to the pure error and the chances that 13.19% of its value also occurred due to noise. The only insignificant model terms were X_2 and X_1X_3 for the 2FI percentage yield model developed (table not shown).

The three parameters selected for PSAC preparation optimization, were all significant in the process as they were all represented in the final significant model's equation; activation temperature had more impact while activation time effect was least. Loss of some volatile matters, gasification of carbon materials, and intercalation of potassium ion into the carbon materials among others contributed to massive weight loss which reflected in the low PSAC yield as compared with that obtained at lower activation temperature. Increase in impregnation ratio also negated yield of PSAC but variation of time was insignificant to the high yield obtained provided the temperature of activation was kept low. The temperature and time (IR = 1.25) 3-D interaction surface plot for the yield is shown in Fig. 2a.

The CCD ANOVA for adsorption of RO16 and RB19 using quadratic regression models suggested, were both significant and had some similar characteristics; their models significant terms were X_1, X_3, X_1^2, X_3^2, X_1X_3, Prob > F of 0.0001 and they all had non-significant lack of fit (table not shown). However, the models lack of fit F-values were 35.10 and 30.89, non-significant lack of fit F-values of 1.66 and 2.47, occurrence of non-significant lack of fit due to noise F-values of 29.50 and 17.22, correlation coefficient value between experimental and predicted R^2 of 0.969 and 0.965 for adsorption of RO16 and RB19, respectively.

Higher adsorption uptake of RO16 and RB19 by PSAC were obtained when high activation temperature was employed in the preparation of PSAC as against the IR dosage; the 3-D surface plot of activation IR and temperature (time = 75 min) for both RO16 and RB19 are shown in Fig. 2b and c, respectively. The porous PSAC obtained was attributed to evacuation of volatile materials and intercalation of potassium ions leading to porosity development at higher activation temperature. Excess activating agent caused by high IR resulted to low adsorption capacity of the adsorbates, this may have caused blockages and possible destruction of the pores of the carbon materials. Excessive amount of KOH used as activating agent was reported to be responsible for further reaction between the KOH and carbon resulting in destruction of pores that were initially developed [30]. The impact of temperature in the development of pores of the PSAC was outstanding in the ANOVA analysis as it had largest F-value of 150.95 and 133.46, for both RO16 and RB19, respectively. The F-values of 23.04 and 24.95 for activation temperature IR interaction were larger than those of other parameters interactions for the two adsorbent ANOVA analyses. Once the optimum time of activation was attained, further increase in time did not promote activation activities, this can be seen in the 3-D surface plot of activation time and temperature (IR = 1.25) for both RO16 and RB19 shown in Fig. 2d and e, respectively.

3.2. Process optimization

The two responses targeted were at variance in terms of the preparations parameters selected for this study. Increase in activation temperature of the process gave better adsorption uptake as against the yield. To study the economic viability of the process, the responses were targeted at maximum while the selected independent parameters ranges were used. The high desirability conditions of 180 mg/g, 10% yield, X_1 = 810 °C, X_2 = 105 min and 0.95 for RO16 adsorption were selected and verified. This gave 178 and 154 mg/g for RO16 and RB19, respectively with 10.05% yield.

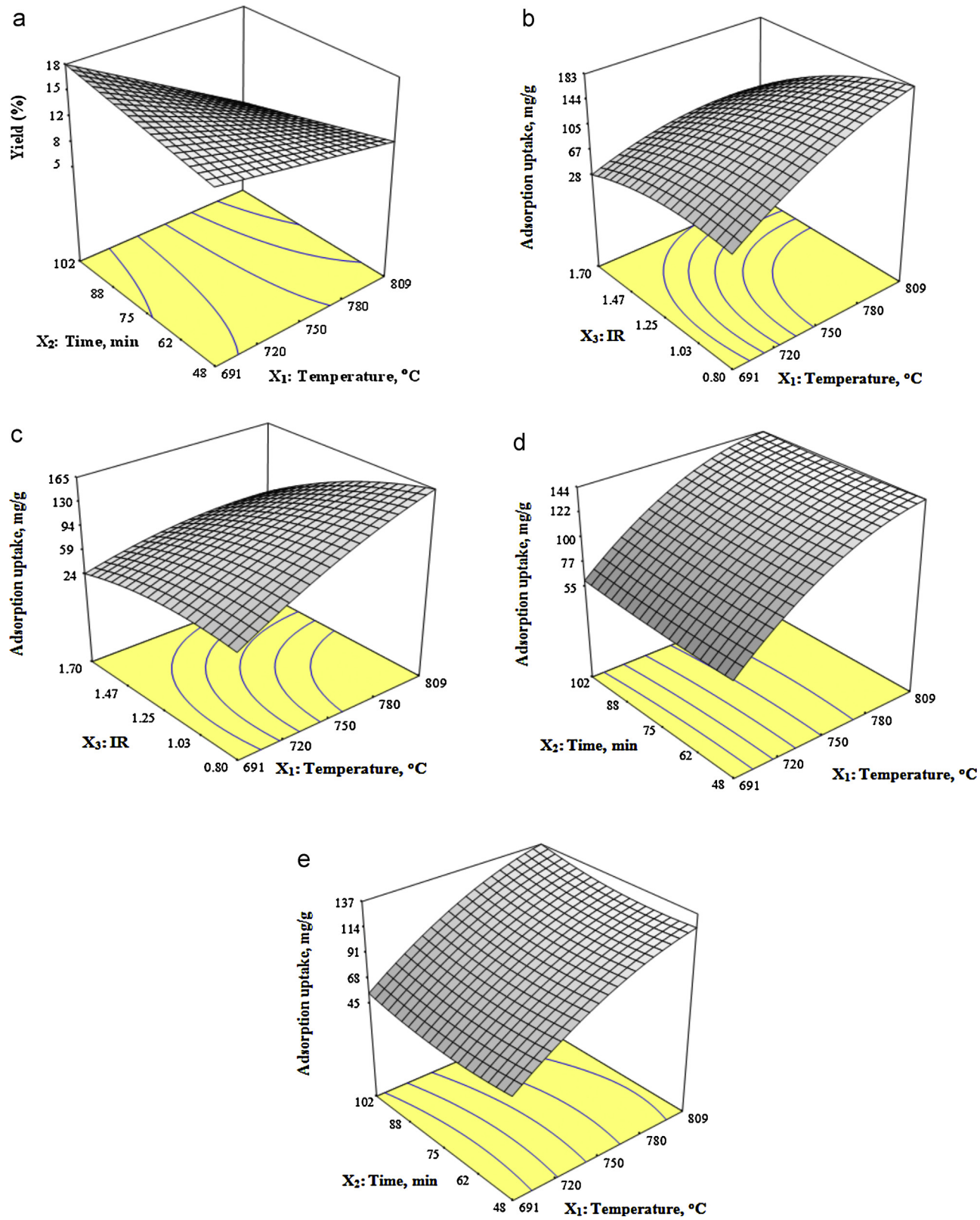

Fig. 2. The 3-dimensional plot of (a) percentage yield (activation time and temperature, IR = 1.25) of PSAC; adsorption uptake (activation temperature and IR, time = 75 min) of PSAC for (b) RO16 and (c) RB19; adsorption uptake (activation time and temperature, IR = 1.25 min) of PSAC for (d) RO16 and (e) RB19.

3.3. Characterization of PS, PSAC and FPSAC

The PS and PSAC BET Langmuir surface areas were 8.57 and 640 m^2/g, and 14.21 and 890 m^2/g, respectively. The PS had total pore volume of 0.003 cm^3/g and pore size of 14.47 nm, while the PSAC had total pore volume of 0.36 cm^3/g and pore size of 2.2 nm. The development of surface area and pore volume was attributed to the gasification reaction of KOH formed and intercalation of the potassium metal ion during pyrolysis process [12,31].

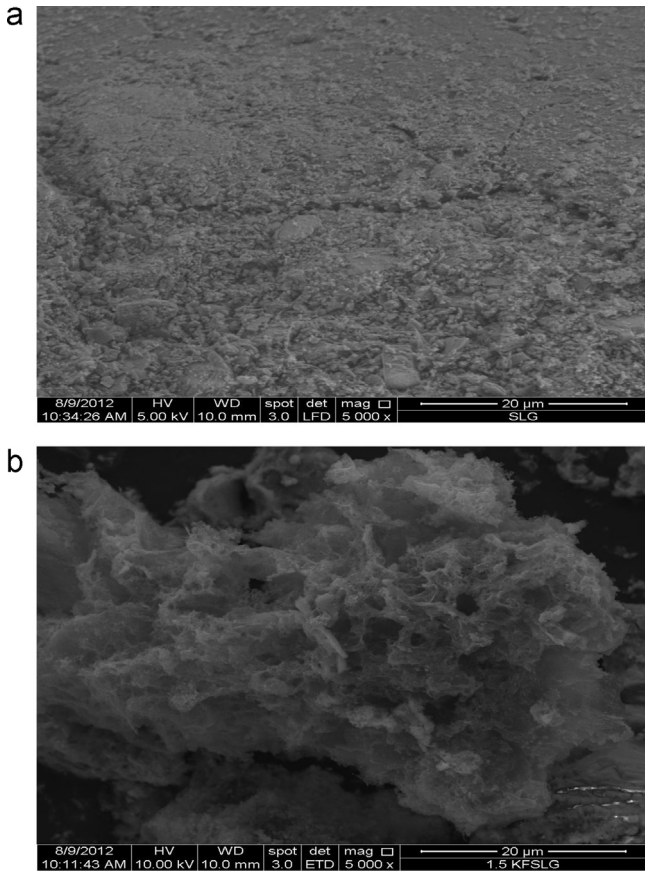

Fig. 3. The morphological structure of (a) raw paper sludge and (b) PSAC (magnification 5k).

The SEM of PS and PSAC are shown in Fig. 3. The raw sludge showed it compacted and dense nature; this could be attributed to lots of volatile components that were still present before activation. Carbonization cum activation processes of PS helped in decomposing some organic matters, intercalation of the potassium ion and loss of some carbon components contributed in the development of pores. This was evident in the morphological structure of the loosed amorphous like structure of PSAC. The SEM of dense and loose structure of raw and carbonized sludge has been reported [32,33].

The points of symmetry on the PS, PSAC and FPSAC spectrums were at wavenumbers 3422, 1622 and 595 cm^{-1} which were assigned to the O–H or N–H, C=C and PO_4^{3-} bends, respectively; this can be seen in Fig. 4a. The bands at 2950 and 887 cm^{-1} on the PS spectrum were found to have disappeared on the PSAC and FPSAC spectrums. It was attributed to the carbonization and activation conditions that the PS was subjected to [34,35]. Significant weakness of bands around 3422 and 1380 cm^{-1} was noticed on both PSAC and FPSAC spectrums when compared with the PS spectrum. Traces of potassium metal residue chemically bound to the pure structures of the adsorbent even after washing may have been responsible. Similar observation has been made on spectrums of activated carbons prepared using KOH as activating agent [35]. Stretching vibrations around 1100 cm^{-1} band width on both the PSAC and FPSAC were attributed to spectrum of CF equivalent to its amount deflagrated [17,36].

The FTIR spectrums of the two adsorbents PSAC and FPSAC revealed presence of numerous functional groups on peaks at different wavenumbers. The spectra had some O–H or N–H functional groups between 3460 and 3250 cm^{-1} which could be attributed to some hydroxyl groups or adsorbed water [37].

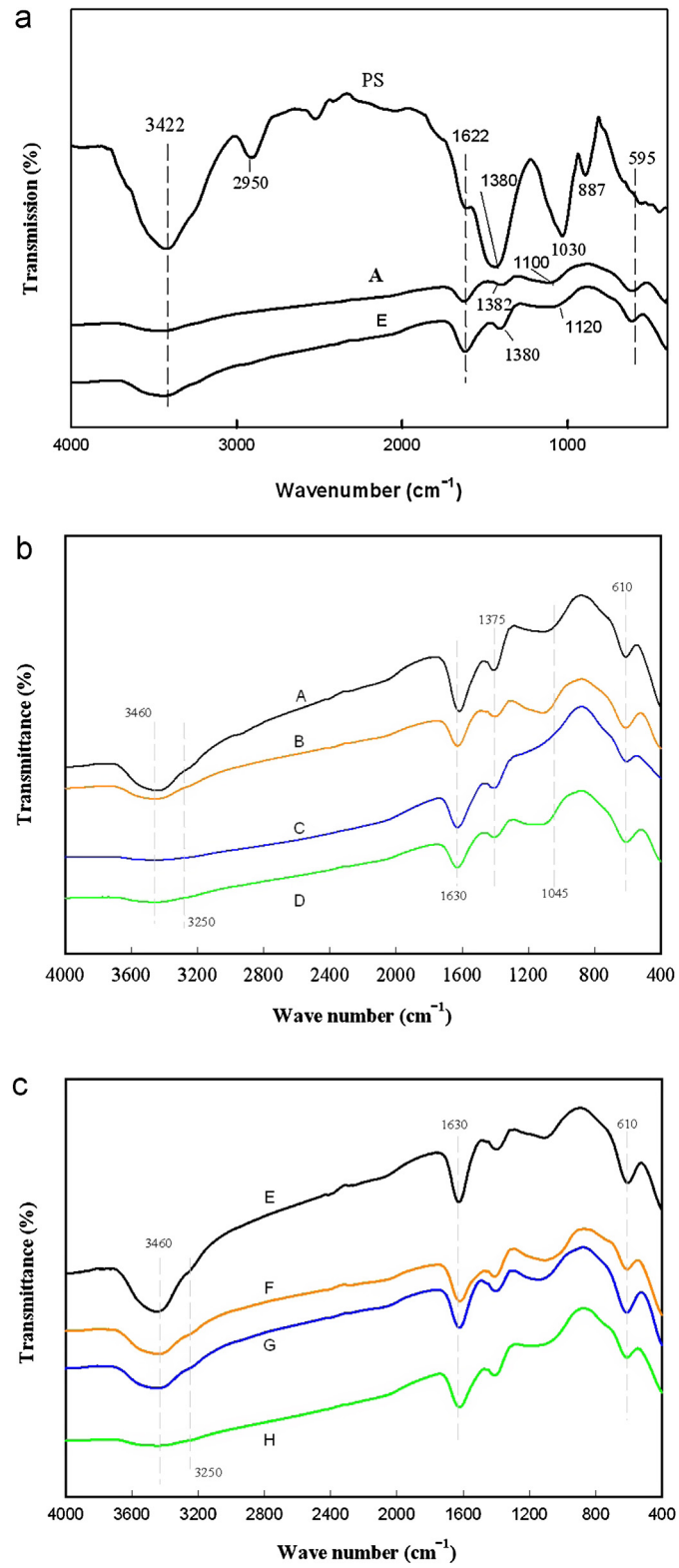

Fig. 4. The FTIR spectrums for (a) PS, A = PSAC, E = FPSAC, (b) A = PSAC, B = PSAC after adsorption of RO16, C = PSAC after RB19 adsorption, D = PSAC after RORBB adsorption; (c) E = FPSAC, F = FPSAC after RO16 adsorption, G = FPSAC after RB19 adsorption, H = FPSAC after RORBB adsorption.

Vibration of some primary amines NH_2 were found at strong peaks on wavenumber 1630 cm^{-1}. Small stretches of some sulfonate SO_2 and sulfur/oxygen bonds S=O were located approximately around wavenumbers 1375 and 1045 cm^{-1} (shoulder at 1150 cm^{-1}) due

to Si–O–Si asymmetric stretch [38]. The presence of compounds of sulfur functional groups was attributed to inherent sulfur contained in the paper sludge as adjudged by the elemental analysis result in Section 2.1. Sulfur was also identified as one of the chemical contents of raw dried paper sludge [33]. Stretches of some inorganic sulfates S–O bends were located around wavenumber 610 cm^{-1}. Although the two adsorbents spectrums had similar characteristics of functional groups, functionalization of PSAC with EDA increased the peaks intensity around 3460 and 1630 cm^{-1} wavenumbers which was synonymous to presence of more N–H and NH_2 functional groups. Functionalization of PSAC with EDA increased presence of nitrogen functionalities which promoted interaction between the $-SO_3^-$ dye ions and protonated $-NH_3^+$ surface of the FPSAC [39]. Similar observation was made when chitosan adsorbent was modified with ethylenediamine [40] and ethylenediamine-modified magnetic chitosan microsphere [25]. The single and binary adsorption of RO16 and RB19 on both PSAC and FPSAC lead to shifts and disappearance of some functional groups on the adsorbents surfaces. The O–H or N–H and some amines functional groups decreased and some disappeared during the adsorption process; the observation was attributed to interaction reaction between the amine groups and sulfonate compounds of the reactive dyes molecules. Disappearance of some O–H groups when MB was adsorbed on waste activated sludge [41] and reduction in peak intensities of some functional groups was observed when Congo red dye was adsorbed on electrocoagulated metals hydroxide sludge [42]. High disappearance of N–H functional groups was more pronounced in the PSAC than FPSAC as observed on spectrums for adsorption of the two adsorbents. Binary adsorption of both RO16 and RB19 on the adsorbents all led to the disappearance of N–H functional groups between 3460 and 3250 cm^{-1}. This can be attributed to limited amine groups required to adsorb both adsorbates in a binary system [41]. The FTIR spectra for PSAC and FPSAC for the single and binary adsorption of RO16 and RB19 are shown in Fig. 4.

The pH zero point of charge (pHzpc) of the PSAC and FPSAC were determined from the plateau like feature of the plots of final pH against initial pH values (figure not shown) as 6.5 and 5.2, respectively. Below the pHzpc of the PSAC and FPSAC, adsorption of both the RO16 and RB19 were favored due to the adsorbents' predisposition to amino groups protonation. This was contrary to repulsion activities between the solution –OH (PSAC and FPSAC) and $-SO_3^-$ (dye molecules) which were dominant at pH values above the pHzpc of the adsorbents [43].

The surface acidity of PSAC and FPSAC determined through Boehm titration [44] were 2.325 and 2.982 mmol/g with their corresponding basicity of 1.785 and 1.213 mmol/g, respectively. Higher adsorption of both RO16 and RB19 on the more acidic surface of FPSAC showed that surface acidity plays an important role in adsorption [45].

3.4. Effect of pH on the adsorption process

Variation of pH 2–12 influenced adsorption of RO16 and RB19 on both surfaces of PSAC and FPSAC (figure not shown). The least and maximum adsorption of the adsorbate occurred at two extremes of the pH varied. At pH 12, the amount of RO16/RB19 adsorbed on PSAC and FPSAC was 47.55/37.09 mg/g and 107.91/91.60 mg/g, respectively. While at pH 2, 347.21/344.85 mg/g were the amounts of RO16/RB19 adsorbed on PSAC and 696.23/689.97 for RO16/RB19 adsorbed on FPSAC. The phenomenon of higher adsorption at lower pH was attributed to dissociation of sulfunate groups (D-SO_3Na) of the anionic dyes (RO16 and RB19) at pH > 1.5 to form anionic ions (D-SO_3^-) and protonation of amine groups ($-NH_3^+$) of the adsorbents surface in the presence of H^+ which led to ionic interaction [46]. Conversely, predominance of $-OH^-$ at higher pH promoted repulsion activities between the adsorbent and the adsorbent. This suggests that the mechanism of adsorption of RO16 and RB19 on both PSAC and FPSAC was also based on electrostatic attraction. The dissociation of the dyes (RO16 and RB19) sulfonate groups (17), protonation of amino groups of PSAC and FPSAC in the presence of H^+ (18) and the electrostatic attraction between the opposite charge ions (resultant anionic ions and protonated amino groups) (19) are given as follows [47]:

$$\text{D-SO}_3\text{Na} \rightarrow \text{SO}_3^- + \text{Na}^+ \tag{17}$$

$$\text{R-NH}_2 + \text{H}^+ \rightleftharpoons \text{R-NH}_3^+ \tag{18}$$

$$\text{R-NH}_3^+(\text{adsorbentsurface}) \rightleftharpoons \text{D-SO}_3^-(\text{dyemolecule}) \tag{19}$$

3.5. Adsorption Isotherm for single adsorption process

Langmuir [48], Freundlich [49] and Temkin and Pyzhev [50] adsorption isotherms were tested to determine the level of fitness to the experimental data generated. Langmuir isotherm model is based on the assumption that there is absence of lateral interaction and steric impediment during adsorption on the adsorbent surface [29], its non-linear model Eq. (20) and the non-linear model equations of Freundlich (21) and Temkin (22) are expressed as:

$$q_e = \frac{q_m C_e b}{(1 + bC_e)} \tag{20}$$

$$q_e = K_F C_e^{1/n} \tag{21}$$

$$q_e = B \ln(k_T C_e) \tag{22}$$

where C_e (mg/L), is the concentration at equilibrium of RO16/RB19 adsorbed; q_e (mg/g), is the experimental adsorption capacity of RO16/RB19 adsorbed on the adsorbent; the monolayer adsorption capacity and affinity of adsorbent toward adsorbate q_m (mg/g) and b (L/g), respectively are the Langmuir constants.

Freundlich constants K_F ((mg/g) $(L/mg)^{1/n}$) and n, are the extent of adsorption and degree of nonlinearity between the adsorption and the solution concentration, respectively. The inverse of n ($1/n$), gives information on the adsorption intensity. Temkin constant k_T (L/mg), is the equilibrium binding constant correlating the maximum binding energy while $B = RT/b_T$; where R is universal gas constant (8.314 J/mol K), T (K) is absolute temperature and b_T (J/mol) is related to heat of adsorption.

The models parameters which were obtained from the plots of equilibrium adsorption against their corresponding concentration are presented in Table 2. Assessment of the models fitness revealed that Langmuir model was the best fit for adsorption RO16 and RB19 on both PSAC and FPSAC as seen by their larger values of R^2 (>0.90) and was closely followed by the Freundlich isotherm model. The affinity for adsorption was consistently decreasing as the temperature decreased as revealed by Langmuir constant b. However, aside the extent of adsorption of Freundlich model which was consistently decreasing with temperature, the adsorption intensity parameter (n) and Temkin model parameters were inconsistent for both adsorbates studies [51].

To affirm the fitness of Langmuir model to the experimental data, an equilibrium parameter expressed as dimensionless constant R_L was evaluated. The outcome of R_L values obtained is interpreted as follows: adsorption systems with $R_L > 1$ (unfavorable), $0 < R_L < 1$ (favorable), $R_L = 1$ (linear) or $R_L = 0$ (irreversible). The characteristic Langmuir model equation is expressed as:

$$R_L = \frac{1}{1 + K_L C_0} \tag{23}$$

Table 2
Langmuir Freundlich and Temkin isotherm models parameters for PSAC and FPSAC.

Adsorbent	Adsorbate	Temp. (°C)	Langmuir parameters			Freundlich parameters			Temkin parameters		
			q_m (mg/g)	b (L/g)	R^2	K_F (mg/g) (L/mg)$^{1/n}$	$1/n$	R^2	k_T (L/mg)	b_T kJ/mol	R^2
PSAC	RO16	30	338.46	0.098	0.99	54.87	0.399	0.98	2.872	48.55	0.92
		40	325.93	0.059	0.98	40.52	0.390	0.87	3.001	37.30	0.84
		50	292.57	0.031	0.95	32.97	0.469	0.94	0.677	43.93	0.90
	RBB19	30	323.00	0.095	0.99	46.08	0.346	0.91	0.994	43.05	0.91
		40	316.36	0.043	0.99	38.75	0.420	0.91	1.654	45.74	0.89
		50	312.21	0.030	0.91	30.64	0.439	0.96	0.553	55.97	0.81
FPSAC	RO16	30	683.46	0.073	0.93	121.09	0.377	0.92	7.997	39.91	0.87
		40	658.23	0.047	0.99	85.21	0.412	0.92	1.548	100.37	0.84
		50	630.31	0.029	0.98	60.66	0.440	0.94	0.693	102.91	0.91
	RBB 19	30	672.53	0.236	0.96	198.29	0.311	0.87	9.791	47.84	0.80
		40	670.75	0.089	0.95	139.57	0.346	0.88	3.165	46.66	0.80
		50	661.01	0.063	0.99	99.78	0.403	0.92	2.369	42.37	0.83

Favorable fitness of Langmuir model to the experimental data was further ascertained as the characteristics constant values were all within the range (0.0640–0.1833 for PSAC and 0.1236–0.4124 for FPSAC) of favorability.

Relatively, the monolayer adsorption capacities of the two adsorbates were close in magnitude, this may be attributed to the similarity in the number of sulfonic and sulfate groups of the two dyes which gave them equal chances of interacting with the adsorbents surfaces. However, the monolayer adsorption capacity of RO16 was higher on the two adsorbents than RB19. This was attributed to easier sorption of smaller molecular sized RO16 as compared with RB19. In a similar scenario, RO16 was found to be more accessible to the pores of Polysulfone-Immobilized Esterified *Corynebacterium glutamicum* adsorbent than RB4 due to its smaller size and single sulfonic acid group [52]. Better adsorption capacity obtained by FPSAC was due to the extra amine groups on its surface (sourced from the functionalization with ethylenediamine) and other numerous functional groups which attracted the sulfonate ($-SO_3^-$) ions of the adsorbate molecules [47,53]. This is also because functionalization of adsorbents enhances swiftness and good selectivity of adsorbate and its mechanical stability [24].

3.6. Binary adsorption studies

The chemical and physical differences between adsorbates molecules in multi-adsorptions systems often promotes competition amongst them on which to be preferentially adsorbed [52,54]. Competitive adsorption between adsorbate molecules affects the affinity between adsorbate and adsorbent surface when compared with single adsorption phenomenon and hence, decreases the adsorption capacity [55]. Higher adsorption was generally observed on FPSAC surface than PSAC as determined by their equilibrium concentrations (table not shown). The highest residual adsorbates concentrations were 40 and 25 mg/L for RO16 adsorption on PSAC and FPSAC, respectively; while RB19 adsorption had about 16 mg/L for PSAC and 9 mg/L for FPSAC as the adsorbate's equilibrium concentrations. Association of each sulfonate group with one amine during adsorption may have given RB19 advantage over RO16 which has two amine groups against one amine of RO16. This observation is similar to that reported on competitive adsorption between RB5 and RO16 [52]. Preference of RB19 adsorption over RO16 was observed during binary adsorption as seen in the θ_2 surface fractional coverage values which were higher than θ_1 values at the best temperature of adsorption even though equal initial concentration of the adsorbates was used. The affinity for adsorption K_L, for RB19 was also higher than RO16 for both PSAC and FPSAC systems evaluated. The binary adsorption model parameters are summarized in Table 3. This is similar to observation made during binary adsorption of Malachite green and Methylene blue [28]. Freundlich, Langmiur and Temkin isotherms for single and binary adsorption of RO16 and RB19 on both adsorbents are presented in Fig. 5.

3.7. Thermodynamics studies

Adsorption thermodynamic parameters enthalpy (ΔH), entropy (ΔS) and Gibbs free energy were evaluated through equilibrium constants-concentration distribution between adsorbent and solution at the various temperatures under study. This can be expressed as follows:

$$K_0 = \frac{C_{ad}}{C_{sol}} \tag{24}$$

where C_{ad} is the concentration of adsorbate (RO16/RB19) adsorbed on PSAC/FPSAC, C_{sol} is concentration of adsorbate in solution at equilibrium condition. The ΔH and ΔS were determined from the slope and intercept of $\ln K_0$ against $1/T$ plots from the van't Hoff

Table 3
Extended Langmuir model parameters for PSAC and FPSAC binary adsorption of RO16 and RB19.

Adsorbent	Dye mix	Temperature (°C)	Experimental parameters		Calculated parameters			
			θ_1	θ_2	$K_{L,1(bin)}$	$K_{L,2(bin)}$	$q_{m(bin)}$	R^2
PSAC	RO16 + RB19	30	0.2993	0.7003	0.0197	0.0496	222.50	0.97
		40	0.3062	0.6938	0.0108	0.0139	195.84	0.98
		50	0.3887	0.6113	0.0083	0.0097	184.24	0.89
FPSAC	RO16 + RB19	30	0.3986	0.6014	0.0265	0.0882	484.63	0.99
		40	0.4747	0.5253	0.0159	0.0350	473.15	0.98
		50	0.5330	0.4670	0.0085	0.0275	418.69	0.96

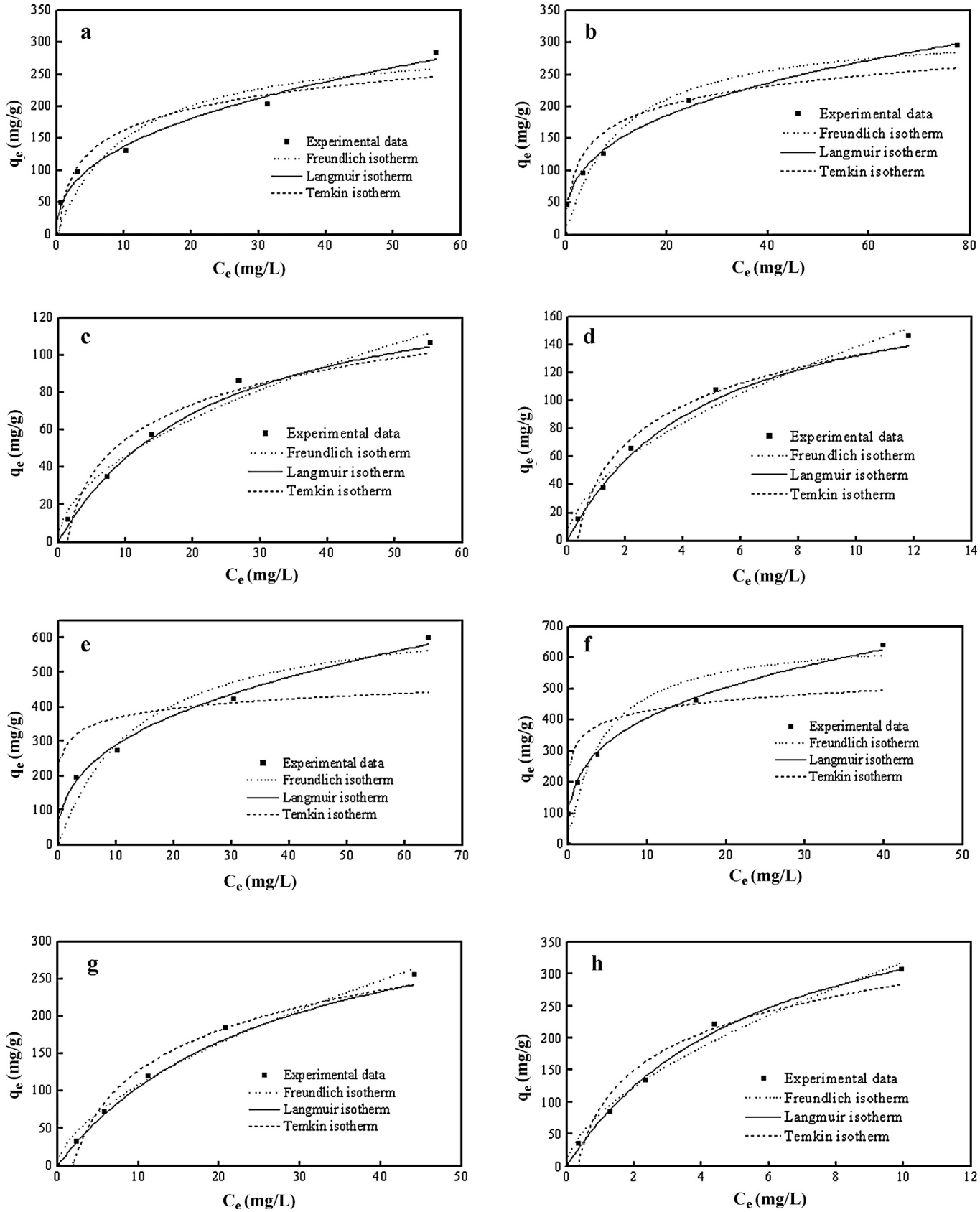

Fig. 5. Freundlich Langmuir and Temkin isotherms for (a) RO16, (b) RB19, (c) RO16 in RORBB and (d) RB19 in RORBB, adsorption on PSAC at 30 °C; (e) RO16, (f) RB19, (g) RO16 in RORBB and (h) RB19 in RORBB, adsorption on FPSAC at 30 °C.

Table 4
Thermodynamic parameters of adsorption of RO16 and RB19 adsorption by PSAC and FPSAC.

Adsorbent	Dye	ΔH (kJ/mol)	ΔS (J/mol K)	ΔG (kJ/mol)		
				30 °C	40 °C	50 °C
PSAC	RO16	−30.22	0.125	−18.07	−8.10	−6.93
PSAC	RB19	−24.38	0.065	−16.46	−10.18	−9.76
FPSAC	RO16	−39.80	0.113	−35.80	−28.42	−20.20
FPSAC	RB19	−39.27	0.224	−38.33	−31.19	−30.61

equation:

$$\ln K_0 = \frac{\Delta S}{R} - \left(\frac{\Delta H}{R}\right)\frac{1}{T} \tag{25}$$

The Gibbs free energy ΔG was calculated using this relationship:

$$\Delta G = -RT \ln K_0 \tag{26}$$

The adsorption process was spontaneous and exothermic in nature since negative values of ΔG and ΔH were obtained. The ΔG values decreased with increase in temperature signifying that lower temperature favored the adsorption process. Lower temperature favored increased affinity and mobilization of the molecules of RO16 and RB19 on both PSAC and FPSAC surfaces. Similar results trend of adsorption phenomenon has been reported [56]. The spontaneity of FPSAC was higher compared with PSAC due to its more negative ΔG values. This increased interaction activities and adsorbate concentration on the adsorbent which promoted better adsorption. The positive values of entropy obtained imply that there was affinity between the RO16 and RB19 molecules and adsorbents and increase in degree of freedom [57]. Higher translational entropy gained by the adsorbed solvent molecules than was lost by the RO16 and RB19 molecules was attributed to the increase in degree of freedom [58]. The adsorption thermodynamic result are summarized in Table 4

3.8. Desorption studies

The two adsorbents showed a common trend of diminishing in adsorption and desorption capacity with increase in reusability. This could be attributed to blockage of some pores by unflinching dye molecules thereby reducing the active sites of the adsorbents. The FPSAC reusability test result was better than PSAC which may be due to more $-NH_2$ groups on its surface that attracted dye molecules to it through Coulombic forces. After the third time of desorption experiment, PSAC percentage adsorption uptake for RO16 and RB19 was 33.85 and 27.97%, respectively; 74.11 and 65.45% were adsorption uptake of RO16 and RB19, respectively on FPSAC (table not shown).

4. Conclusion

The study shows that activated carbon can be activated chemically using potassium fluoride as activating agent as demonstrated using paper sludge precursor. This is evident from the BET characterization analysis for surface area and porosity of PSAC. Functionalization of the PSAC improved the adsorption efficiency of RO16 and RB19 for both single and binary adsorption systems. The adsorbents (PSAC and FPSAC) are good for adsorption of reactive dyes and can be reused.

Acknowledgement

Authors acknowledge the research grant provided by the Universiti Sains Malaysia under the Postgraduate Research Grant Scheme (PRGS) (Project no. 1001/PJKIMIA/8045026).

References

[1] M.A.M. Salleh, D.K. Mahmoud, W.A.W.A. Karim, A. Idris, Desalination 280 (2011) 1.
[2] S.B. Uma, Y.C. Sharma, Journal of Industrial and Engineering Chemistry 19 (2013) 1099.
[3] M. Auta, B.H. Hameed, Chemical Engineering Journal 171 (2011) 502.
[4] T.-Y. Kim, S.-S. Park, S.-Y. Cho, Journal of Industrial and Engineering Chemistry 18 (2012) 1458.
[5] D. Fytili, A. Zabaniotou, Renewable Sustainable Energy Reviews 12 (2008) 116.
[6] C. Ignacio, R. Belen, H. Jens, Technology and Environmental Policy on Urban Wastewater Treatment Directives 91/271/EEC – A Case Study of Spain, Institute for Propective Technological Studies (IPTS), 2000, p. 114.
[7] K.M. Smith, G.D. Fowler, S. Pullket, N.J.D. Graham, Water Research 43 (2009) 2569.
[8] M. Auta, B.H. Hameed, Chemical Engineering Journal 175 (2011) 233.
[9] M.A. Lillo-Ródenas, A. Ros, E. Fuente, M.A. Montes-Morán, M.J. Martin, A. Linares-Solano, Chemical Engineering Journal 142 (2008) 168.
[10] A. Ros, M.A. Lillo-Rodenas, E. Fuente, M.A. Montes-Moran, M.J. Martin, A. Linares-Solano, Chemosphere 65 (2006) 132.
[11] H.-Y. Kang, S.-S. Park, Y.-S. Rim, Korean Journal of Chemical Engineering 23 (2006) 948.
[12] B. Viswanathan, P. Indra Neel, T.K. Varadarajan, Methods of Activation and Specific Applications of Carbon Materials, Chennai, India, (2009), p. 160.
[13] J.I. Hayashi, T. Horikawa, I. Takeda, K. Muroyama, F. Nasir Ani, Carbon 40 (2002) 2381.
[14] J.H. Zhu, Y. Chun, Y. Qin, Q.-H. Xu, Microporous and Mesoporous Materials 24 (1998) 19.
[15] M.-J. Jung, J.W. Kim, J.S. Im, S.-J. Park, Y.-S. Lee, Journal of Industrial and Engineering Chemistry 15 (2009) 410.
[16] S. Afzal, A. Rahimi, M.R. Ehsani, H. Tavakoli, Journal of Industrial and Engineering Chemistry 16 (2010) 147.
[17] G.D. Del Cul, L.D. Trowbridge, L.M. Toth, J.N. Fiedor, Journal of Fluorine Chemistry 101 (2000) 137.
[18] A.S. Haja Hameed, G. Ravi, P. Ramasamy, Journal of Crystal Growth 229 (2001) 547.
[19] C. Xu, J. Sun, B. Zhao, Q. Liu, Applied Catalysis B: Environmental 99 (2010) 111.
[20] R.L. Radovic, Chemistry and Physics of Carbon, CRC Press, 6000 Broken Sound Parkway NW, FL 33487-2742, Suite 300 Boca Raton, 2008p. 1.
[21] E. Raymundo-Piñero, P. Azaïs, T. Cacciaguerra, D. Cazorla-Amorós, A. Linares-Solano, F. Béguin, Carbon 43 (2005) 786.
[22] M.J. Belzunce, S. Mendioroz, J. Haber, Clays Clay Minerals 46 (1998) 603.
[23] N.R. Khalili, J.D. Vyas, W. Weangkaew, S.J. Westfall, S.J. Parulekar, R. Sherwood, Separation and Purification Technology 26 (2002) 295.
[24] P.K. Jal, S. Patel, B.K. Mishra, Talanta 62 (2004) 1005.
[25] L. Zhou, Z. Liu, J. Liu, Q. Huang, Desalination 258 (2010) 41.
[26] T.S. Anirudhan, T.A. Rauf, Journal of Industrial and Engineering Chemistry (2013), http://dx.doi.org/10.1016/j.jiec.2013.2001.2036.
[27] I.A.W. Tan, A.L. Ahmad, B.H. Hameed, Chemical Engineering Journal 137 (2008) 462.
[28] A. Kurniawan, H. Sutiono, N. Indraswati, S. Ismadji, Chemical Engineering Journal 189–190 (2012) 264.
[29] K.H.K. Choy, J.F. Porter, G. McKay, Journal of Chemical & Engineering Data 45 (2000) 575.
[30] B.H. Hameed, I.A.W. Tan, A.L. Ahmad, Journal of Hazardous Materials 164 (2009) 1316.
[31] T. Tay, S. Ucar, S. Karagöz, Journal of Hazardous Materials 165 (2009) 481.
[32] W.-H. Li, Q.-Y. Yue, B.-Y. Gao, Z.-H. Ma, Y.-J. Li, H.-X. Zhao, Chemical Engineering Journal 171 (2011) 320.
[33] Z.-H. Pan, J.-Y. Tian, G.-R. Xu, J.-J. Li, G.-B. Li, Water Research 45 (2011) 819.
[34] A.-N.A. El-Hendawy, Applied Surface Science 255 (2009) 3723.
[35] H. Deng, G. Li, H. Yang, J. Tang, J. Tang, Chemical Engineering Journal 163 (2010) 373.
[36] J. Li, Q. Wang, C. Su, Q. Chen, European Polymer Journal 43 (2007) 2928.
[37] E. Demirbas, N. Dizge, M.T. Sulak, M. Kobya, Chemical Engineering Journal 148 (2009) 480.
[38] Y. Zhao, Y. Shen, L. Bai, Journal of Colloid and Interface Science 379 (2012) 94.
[39] M.S. Shafeeyan, W.M.A.W. Daud, A. Houshmand, A. Shamiri, Journal of Analytical and Applied Pyrolysis 89 (2010) 143.
[40] X.-Y. Huang, J.-P. Bin, H.-T. Bu, G.-B. Jiang, M.-H. Zeng, Carbohydrate Polymer 84 (2011) 1350.
[41] K. Gobi, M.D. Mashitah, V.M. Vadivelu, Chemical Engineering Journal 171 (2011) 1246.
[42] A.K. Golder, A.N. Samanta, S. Ray, Chemical Engineering Journal 122 (2006) 107.
[43] F. Pereira de Sá, B.N. Cunha, L.M. Nunes, Chemical Engineering Journal 215–216 (2013) 122.
[44] A.M. Oickle, S.L. Goertzen, K.R. Hopper, Y.O. Abdalla, H.A. Andreas, Carbon 48 (2010) 3313.

[45] N.N. Nassar, A. Hassan, P. Pereira-Almao, Journal of Colloid and Interface Science 360 (2011) 233.
[46] R. Cheng, S. Ou, M. Li, Y. Li, B. Xiang, Journal of Hazardous Materials 172 (2009) 1665.
[47] L. Zhou, J. Jin, Z. Liu, X. Liang, C. Shang, Journal of Hazardous Materials 185 (2011) 1045.
[48] I. Langmuir, Journal of American Chemical Society (1916) 2221.
[49] H.M.F. Freundlich, Journal of Physical Chemistry 57 (1906) 385.
[50] M.J. Temkin, V. Pyzhev, Acta Physiochimica USSR 12 (1940) 217.
[51] H. Zheng, D. Liu, Y. Zheng, S. Liang, Z. Liu, Journal of Hazardous Materials 167 (2009) 141.
[52] K. Vijayaraghavan, S.W. Won, Y.S. Yun, Industrial, Engineering Chemical Research 47 (2008) 3179.
[53] Z. Aksu, S. Tezer, Process Biochemistry 36 (2000) 431.
[54] K.H.K. Choy, S.J. Allen, G. McKay, Adsorption 11 (2005) 255.
[55] N. Atar, A. Olgun, S. Wang, S. Liu, Journal of Chemical & Engineering Data 56 (2011) 508.
[56] P. Saha, S. Chowdhury, S. Gupta, I. Kumar, Chemical Engineering Journal 165 (2010) 874.
[57] M. Auta, B.H. Hameed, Journal of Industrial and Engineering Chemistry 19 (2013) 1153.
[58] G.Z. Kyzas, N.K. Lazaridis, A.C. Mitropoulos, Chemical Engineering Journal 189–190 (2012) 148.